Analysis of Mach-Zehnder Interferometer Free Spectral Range in SIO Photonics

Farhad Majdeteimouri Farhad@infleqtion.com
Infleqtion, Boulder, Colorado, United States

***Abstract*—The goal of this paper is to design, simulate, layout and analyze the performance of an SOI Mach-Zehnder Interferometer (MZI). The design includes several implementations of the same MZI circuit varying the optical path length different between the 2 arms of the interferometer to explore and verify the Free Spectral Range (FSR) of the interferometer. This effort will explore both TE and TM modes in a Silicon slab waveguide with 220nm height and 500nm width.**

I. INTRODUCTION

Integrated photonics is a rapidly evolving field contributing to many areas of science and technology including quantum computing, telecommunication, sensing and metrology. This massive adoption is due to their compact size, low power consumption and high bandwidth. A widely used circuit in integrated photonics is the interferometer. These circuits are powerful tools for precise measurement of optical phase in response to very small perturbations in the optical path length; hence, they are used in temperature, strain, displacement and vibration sensing applications. The goal of this paper is to simulate, design, layout, fabricate and analyze the performance of a Silicon-based integrated photonic Mach-Zehnder interferometer (MZI).

II. THEORY

Figure 1 shows the schematic of a basic Mach-Zehnder interferometer. Here the light splits into to arms using a beam splitter. After bouncing off a mirror the 2 arms are recombined using a second beam splitter. The interference fringes are then detected on the output ports of that beam splitter.

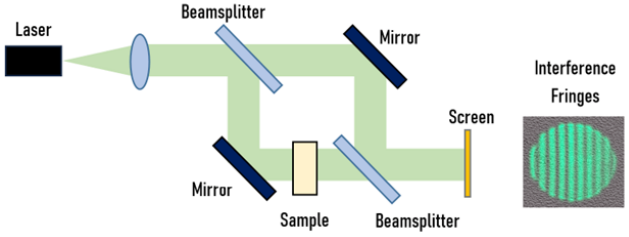

Fig. 1. A simple Mach-Zehnder Interferometer [1].

There are 2 separate versions of the MZI based on the optical path difference of the 2 arms. If both arms go through the same optical path length, then the interferometer is balanced, otherwise it is referred to as an imbalanced interferometer.

The imbalanced version is useful in measuring the refractive index of a material or measure and analyzing the change in the index of refraction of a sample of a material due to temperature variations or vibration.
The output intensity of an imbalanced interferometer is:

$$I_o = \frac{I_i}{2}\left[1 + \cos(\beta.\Delta L)\right] \quad (1)$$

where I_o is the output intensity at one of the output ports,
I_i is the intensity of the input light,
ΔL is the optical path difference between the arms of the interferometer,
β is the propagation constant of light given as

$$\beta = \frac{2\pi n}{\lambda} \quad (2)$$

where n is the index of refraction of the medium.
And λ is the wavelength of light. To make use of the interferometer we need to understand how the output intensity varies with wavelength. This is captured in a parameter called the Free Spectral Range (FSR). The FSR provides an equation that relates the spacing between 2 adjacent peaks in the intensity profile vs wavelength and group index:

$$FSR = \Delta\lambda = \frac{\lambda^2}{\Delta L.n_g} \quad (3)$$

where n_g is the group index.
In the following sections we will examine this formula by simulating the interferometer using the Ansys Lumerical software. Specifically, we will calculate the group index from the experimentally measure FSR using this relationship derived from (2):

$$n_g = \frac{\lambda^2}{\Delta L.FSR} \quad (4)$$

III. MODELING AND SIMULATION

To implement the MZI on a silicon chip we need a few components, this includes waveguides, splitters/combiners and fiber grating couplers.
Our 1st step is to model and simulate the behavior of the waveguide. We will do this using Lumerical MODE.
For this paper we will investigate waveguides with a standard 220nm height and 500nm width. At this width there are only 2 allowed modes, one TE and one TM as shown in (2).

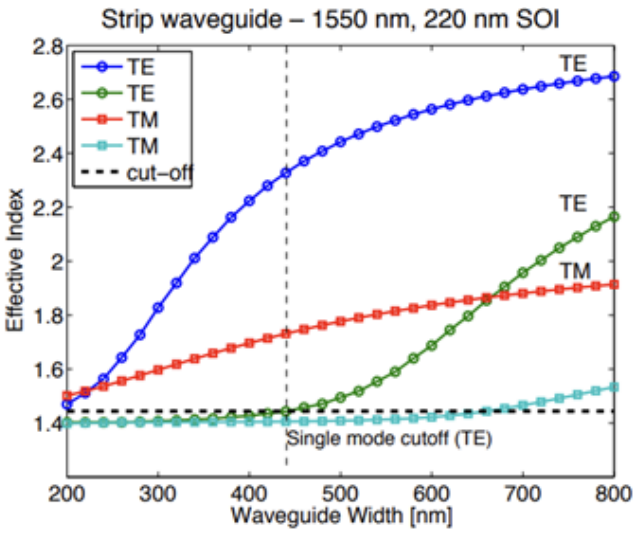

Fig. 2. SOI Strip waveguide, 1550 nm, 220x500nm, allowed modes [2].

The effective index along with the group index for these modes at 1.5um are shown in table (1).

TABLE I
WAVEGUIDE PROPERTIES

MODE	EFFECTIVE INDEX	GROUP INDEX	TE POLARIZATION FRACTION (%)
TE	2.503	4.196	99
TM	1.836	4.007	4

Next we will sweep the wavelength from 1.5 to 1.6 um to see how the effective index varies for each mode. The results are shown in (3).

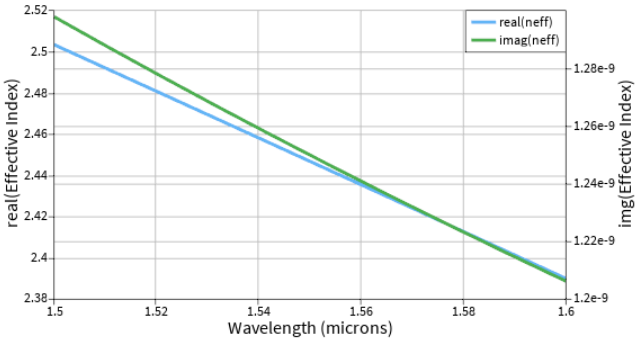

a. Transverse Electric (TE)

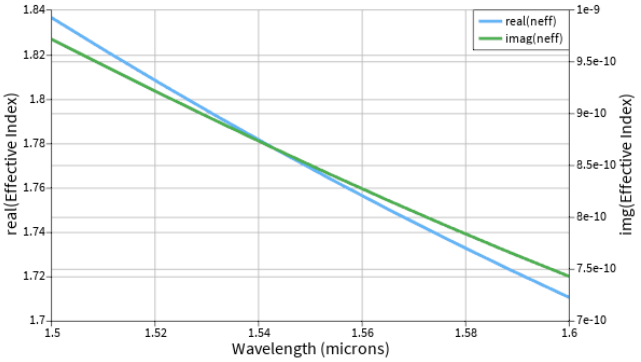

b. Transverse Magnetic (TM)

Fig. 3. Variation of the effective index for the 1st TE and TM modes in a 200x500nm slab waveguide.

A. Compact Model

The effective index variation with wavelength can be captured in compact analytical form using a 2nd order Tylor expansion around the sweep central frequency:

$$n_{eff}(\lambda) = n_1 + n_2(\lambda - \lambda_0) + n_3(\lambda - \lambda_0)^3 \qquad (5)$$

The coefficients of this equation are related to conventional parameter at wavelength λ_0 according to the following relationships:

$$n_{eff} = n_1 \qquad (6)$$

$$n_g = n_1 - n_2.\lambda_0 \qquad (7)$$

$$D = -2.\lambda_0.\frac{n_3}{c} \quad [\text{s/m2}] \qquad (8)$$

Extracting sweep data form Lumerical MODE and using a fit algorithm in MATLAB we can calculate the coefficients for the compact model for each mode. These are shown in table (2).

TABLE II
WAVEGUIDE COMPACT MODEL COEFFICIENTS

MODE	N1	N2	N3
TE	2.446	-1.133	0.043
TM	1.768	-1.258	1.913

B. Intensity Plots

In this section we will explore the intensity plots for each mode to demonstrate that the electric and magnetic fields within each mode are oscillating in the appropriate orientation according to the mode, TE vs TM.

C. Transverse Electric (TE)

Figure (5) shows the total electric field intensity along with its components along the x, y and z coordinates.

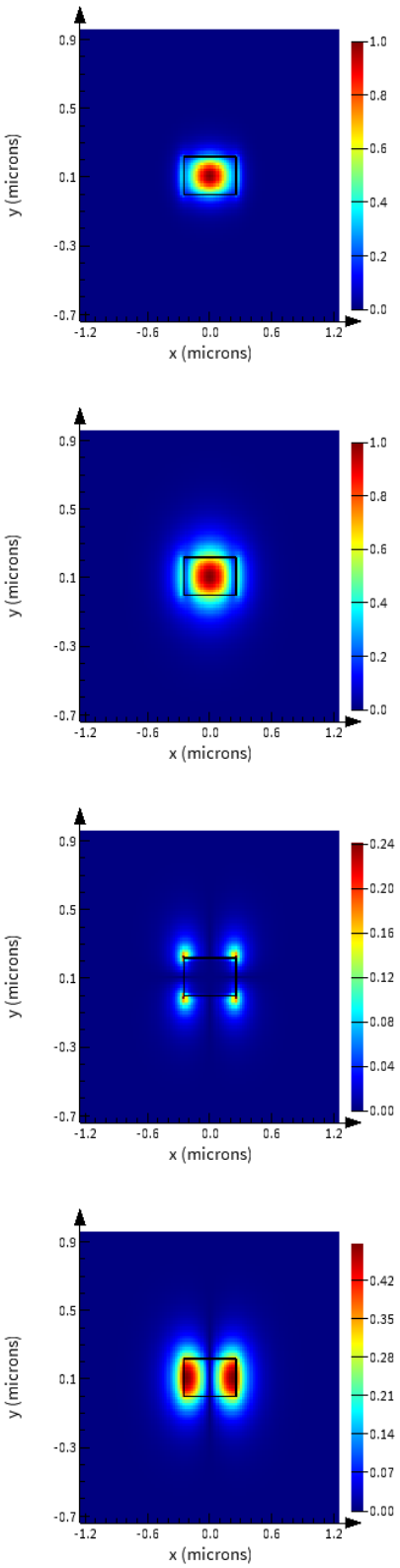

Fig. 4. The electric field distribution for the TE mode: (a) magnitude, (b) component along x, (c) components along y, and (d) component along the z axis.

As you can see from these plots the electric field is mainly osculating in the x direction (transverse) with very small contributions in the y and z.

The electric field distribution for the TM mode is plotted in figure (6).

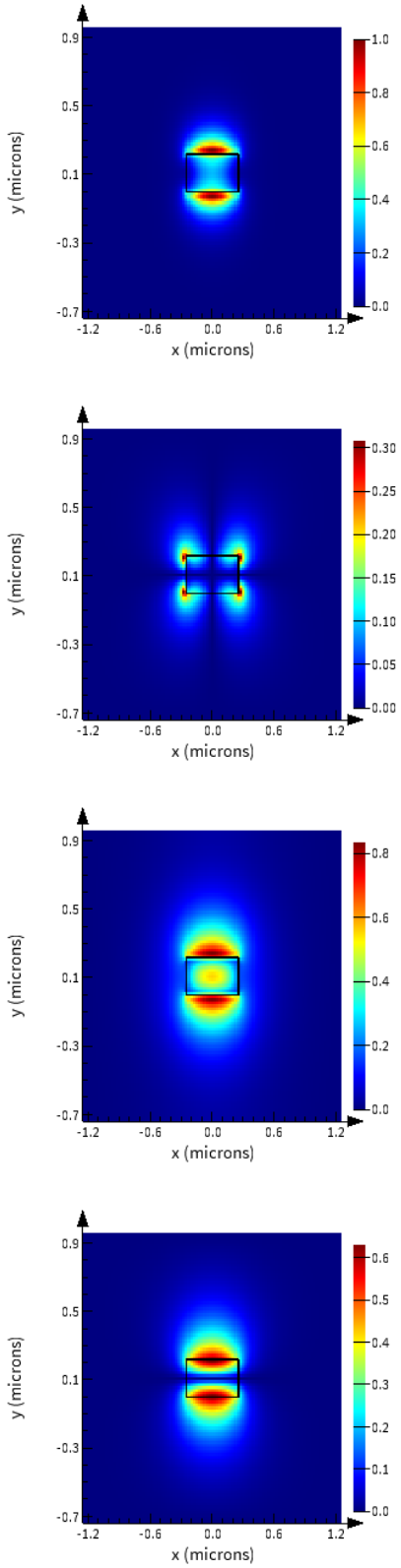

Fig. 5. The electric field distribution for the TM mode: (a) magnitude, (b) component along x, (c) components along y, and (d) component along the z axis.

In this case the largest component is in the y direction, perpendicular to the direction of propagation (x in this model).

D. MZI Circuit

Next, let's turn our attention to the MZI circuit. To implement the circuit we need a few components, 2 waveguides, 2 Y-branches, and 2 Bragg Grating Couplers. The schematic of our MZI circuit in Lumerical INTERCONNET is shown in (5). For Bragg Grating Couplers we use a model provided by the SiEPIC library which includes the device S-parameters. Similarly, we use one of the Y-branch models provided with the course material. For the waveguides we use the model we developed in Lumerical MODE and analyzed in the previous section.

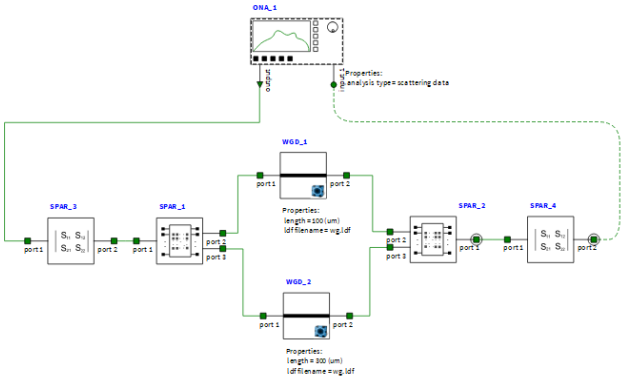

Fig. 6. Circuit schematic for simple Mach-Zehnder Interferometer implemented using Lumerical INTERCONECT.

For our design we explore 3 different values for Optical Path Difference (ΔL) between the 2 arms of the MZI. These values along with the expected FSR are shown in table III.

TABLE III
MZI DESIGN CONFIGURATIONS

	ΔL (μM)	FSR (NM)
1	25	22.81
2	50	11.44
3	100	5.72

Here is

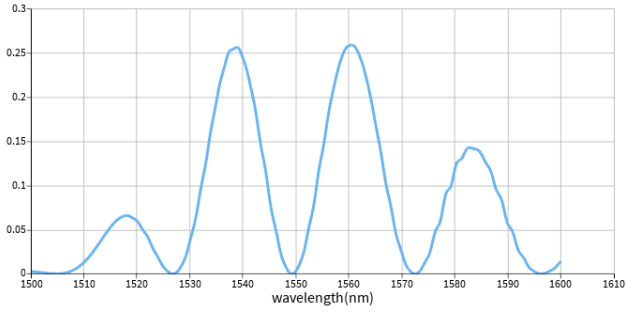

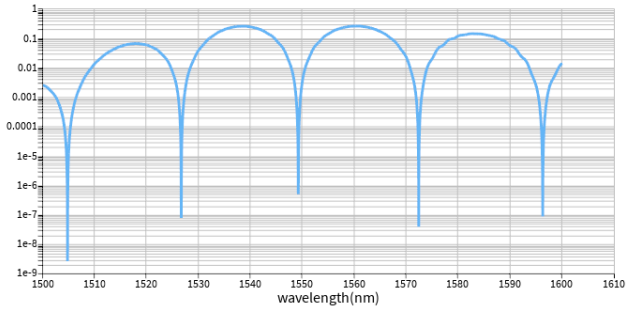

a. ΔL = 25μm

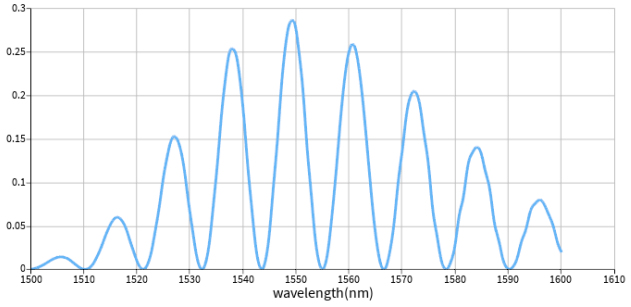

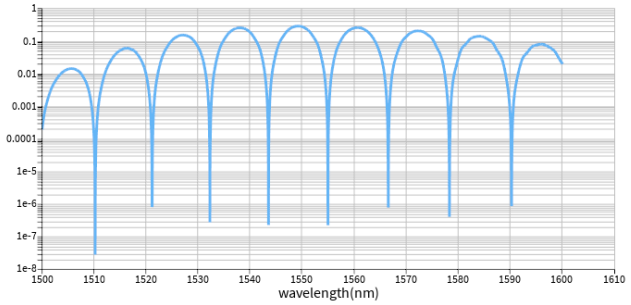

b. ΔL = 50μm

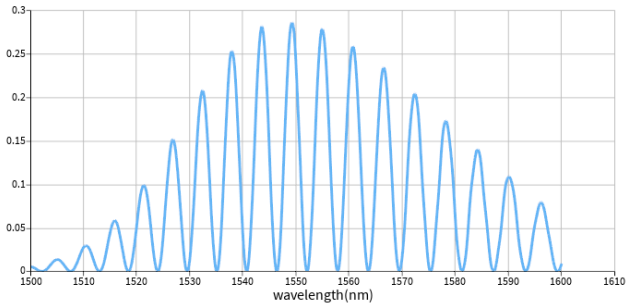

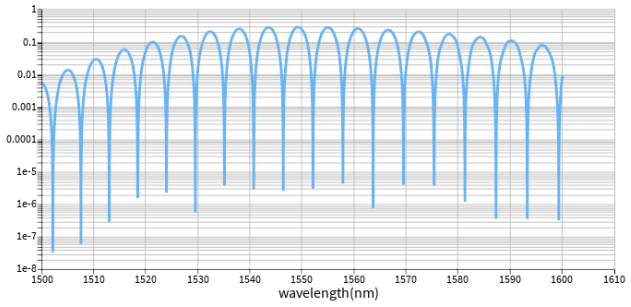

c. ΔL = 100μm

Fig. 7. Transmission spectrum, linear and log scale, of the MZI for the parameters shown in Table I: (a) ΔL = 25μm, (b) ΔL = 50μm, (c) ΔL = 100μm

We will use equation (3) to calcualte the group index based on our measuremnet results in section V.

IV. LAYOUT

The circuit layout was performed using the KLayout package utilizing the SiEPIC library as shown in figure 8.

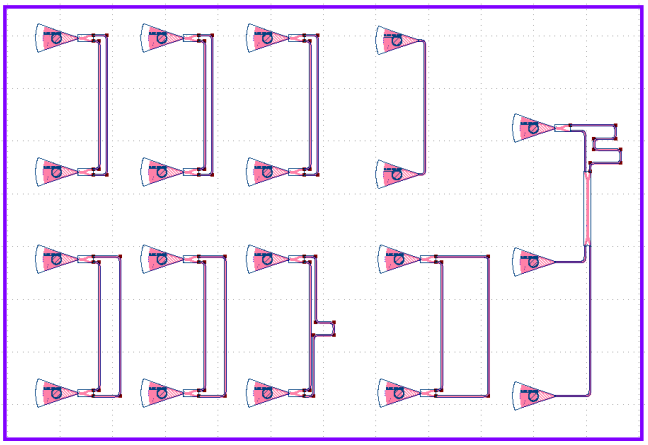

Fig. 8. Circuit layout in KLayout, the floor plan is 605 um (width) x 410 um (height).

The floorplan is set to 605 um (width) x 410 um (height) per the constraints provided by the fab house. All the grating couplers are facing left to comply with the test setup at UBC. Also, the spacing between the grating couplers for each circuit is set to 127 um, again as required by the test setup.

The design includes a de-embedding (loop back) circuit to provide a calibration tool to subtract the insertion loss of the fiber gratings.

V. FABRICATION

The fabrication for this course was performed at the Applied Nanotools and/or Washington Nanofabrication Facility using Electron Beam Lithography.

A. Applied Nanotools, Inc. NanoSOI process

The photonic devices were fabricated using the NanoSOI MPW fabrication process by Applied Nanotools Inc. (http://www.appliednt.com/nanosoi; Edmonton, Canada) which is based on direct-write 100 keV electron beam lithography technology. Silicon-on-insulator wafers of 200 mm diameter, 220 nm device thickness and 2 μm buffer oxide thickness are used as the base material for the fabrication. The wafer was pre-diced into square substrates with dimensions of 25x25 mm, and lines were scribed into the substrate backsides to facilitate easy separation into smaller chips once fabrication was complete. After an initial wafer clean using piranha solution (3:1 H2SO4:H2O2) for 15 minutes and water/IPA rinse, hydrogen silsesquioxane (HSQ) resist was spin-coated onto the substrate and heated to evaporate the solvent. The photonic devices were patterned using a JEOL JBX-8100FS electron beam instrument at The University of British Columbia. The exposure dosage of the design was corrected for proximity effects that result from the backscatter of electrons from exposure of nearby features. Shape writing order was optimized for efficient patterning and minimal beam drift. After the e-beam exposure and subsequent development with a tetramethylammonium sulfate (TMAH) solution, the devices were inspected optically for residues and/or defects. The chips were then mounted on a 4” handle wafer and underwent an anisotropic ICP-RIE etch process using chlorine after qualification of the etch rate. The resist was removed from the surface of the devices using a 10:1 buffer oxide wet etch, and the devices were inspected using a scanning electron microscope (SEM) to verify patterning and etch quality. A 2.2 μm oxide cladding was deposited using a plasma-enhanced chemical vapour deposition (PECVD) process based on tetraethyl orthosilicate (TEOS) at 300ºC. Reflectrometry measurements were performed throughout the process to verify the device layer, buffer oxide and cladding thicknesses before delivery.

B. Washington Nanofabrication Facility (WNF) process

The devices were fabricated using 100 keV Electron Beam Lithography [3]. The fabrication used silicon-on-insulator wafer with 220 nm thick silicon on 3 μm thick silicon dioxide. The substrates were 25 mm squares diced from 150 mm wafers. After a solvent rinse and hot-plate dehydration bake, hydrogen silsesquioxane resist (HSQ, Dow-Corning XP-1541-006) was spin-coated at 4000 rpm, then hotplate baked at 80 °C for 4 minutes. Electron beam lithography was performed using a JEOL JBX-6300FS system operated at 100 keV energy, 8 nA beam current, and 500 μm exposure field size. The machine grid used for shape placement was 1 nm, while the beam stepping grid, the spacing between dwell points during the shape writing, was 6 nm. An exposure dose of 2800 μC/cm2 was used. The resist was developed by immersion in 25% tetramethylammonium hydroxide for 4 minutes, followed by a flowing deionized water rinse for 60 s, an isopropanol rinse for 10 s, and then blown dry with nitrogen. The silicon was removed from unexposed areas using inductively coupled plasma etching in an Oxford Plasmalab System 100, with a chlorine gas flow of 20 sccm, pressure of 12 mT, ICP power of 800 W, bias power of 40 W, and a platen temperature of 20 °C, resulting in a bias voltage of 185 V. During etching, chips were mounted on a 100 mm silicon carrier wafer using perfluoropolyether vacuum oil. Cladding oxide was deposited

using plasma enhanced chemical vapor deposition (PECVD) in an Oxford Plasmalab System 100 with a silane (SiH4) flow of 13.0 sccm, nitrous oxide (N2O) flow of 1000.0 sccm, high-purity nitrogen (N2) flow of 500.0 sccm, pressure at 1400mT, high-frequency RF power of 120W, and a platen temperature of 350C. During deposition, chips rest directly on a silicon carrier wafer and are buffered by silicon pieces on all sides to aid uniformity.

VI. Experiment Data

To characterize the devices, a custom-built automated test setup [4, 8] with automated control software written in Python was used [5]. An Agilent 81600B tunable laser was used as the input source and Agilent 81635A optical power sensors as the output detectors. The wavelength was swept from 1500 to 1600 nm in 10 pm steps. A polarization maintaining (PM) fiber was used to maintain the polarization state of the light, to couple the TE polarization into the grating couplers [6]. A 90º rotation was used to inject light into the TM grating couplers [6]. A polarization maintaining fiber array was used to couple light in/out of the chip [7].

The results for the measured MZI at the output of each circuit was provided in 2 formats, a CSV file and a Matlab data file (.mat). The analysis involved several steps all performed in Matlab.

The 1st step was to extract the wavelength and the MZI output power from the MAT file. The MAT file included 5 arrays, one for wavelength and 4 for the fiber gratings, even if not all 4 were present in a circuit. Figure 9 shows the output of the 2nd 100um delay MZI circuit.

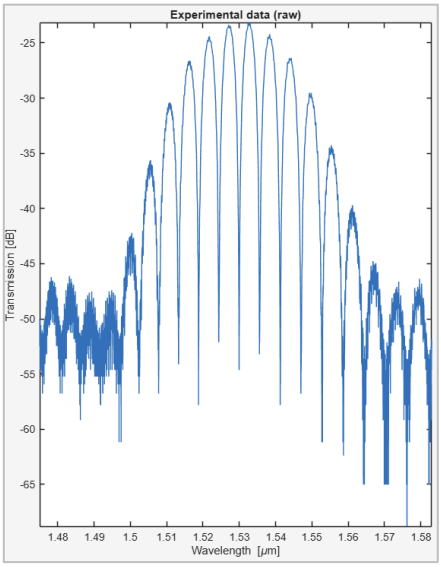

Fig. 9. Raw MZI spectrum from 'FarhadM_MZI1002', this circuit has ΔL = 100 μm.

The next step was to use the loop back spectrum from the calibration circuit to remove the effects of the grating couplers from the MZI spectrum. The loopback output along with a polynomial fit is shown in figure 10.

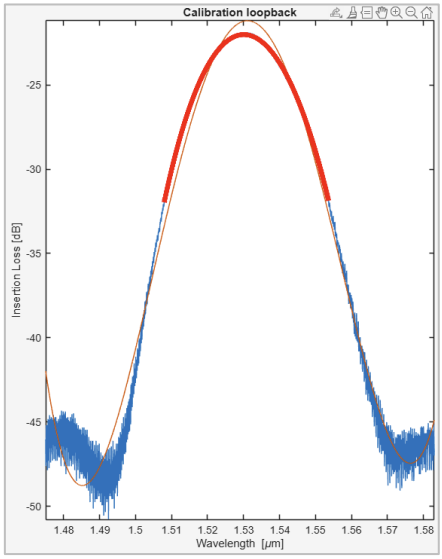

Fig. 10. The loopback output (blue), its polynomial fit (thin red) and the low noise portion of the polynomial fit (thick red).

The red curve in figure 10 represents a subsection of the polynomial fit where the amplitude is within 10 dB of the peak resulting in a stable version of the data with much lower noise.

In the next step is loop back fit will be subtracted from the original MZI signal to eliminate the effects of the grating couplers on the MZI output. The result is shown in figure 11.

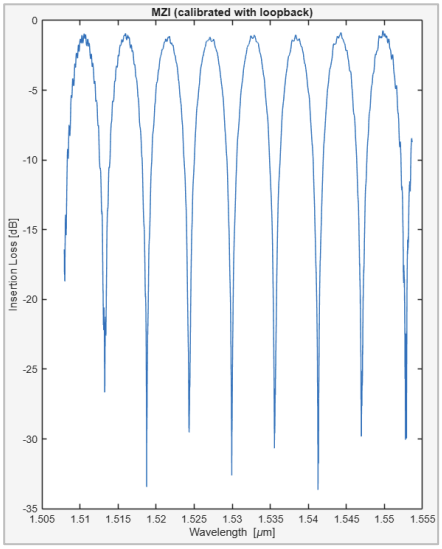

Fig. 11. Process MZI spectrum; the insertion loss due to the fiber gratings are removed from the MZI spectrum by subtracting the loop back spectrum.

At this point the MZI data is ready for fitting, to perform the fit we need to find appropriate initial values to ensure the fitting algorithm converges without falling into a local minima and missing the global one. This is achieved by using autocorrelation on the MZI spectrum. The autocorrelation results is shown in figure 12.

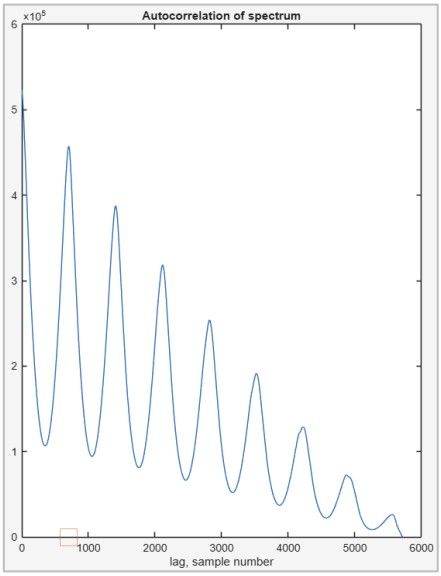

Fig. 12. The MZI autocorrelation. This provides the FSR and an initial value for performing fit.

The position of the 1st peak in the autocorrelation plot is marked on the x axis by a red square. This value is also the FSR of the MZI spectrum. Using this value, we use the MZI transfer function (9) to start the fit.

$$F = 10\,log_{10}\left(\frac{1}{4}\left|1+\exp\left[-i\frac{2\pi n_{eff}}{\lambda}\Delta L-\frac{\alpha\Delta L}{2}\right]\right|^2\right)+b \quad (9)$$

The initial value based on the FSR derived from autocorrelation is shown in figure 13. As evident on this plot the periodicity is a close match, but the offset is obviously present.

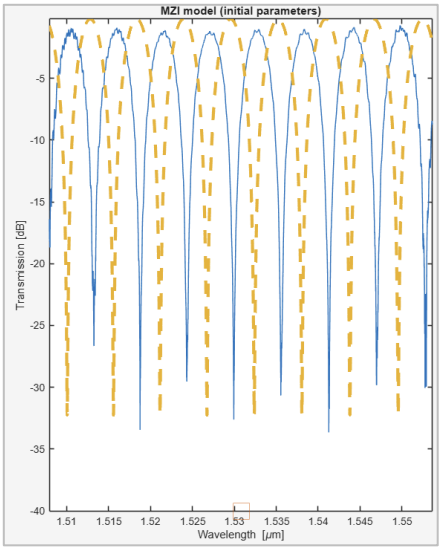

Fig. 13. Initial fit function overlayed on top of the MZI spectrum. The offset needs to be adjusted via optimization (fitting).

The next step is to run the fitting algorithm and plot the results as shown in figure 14.

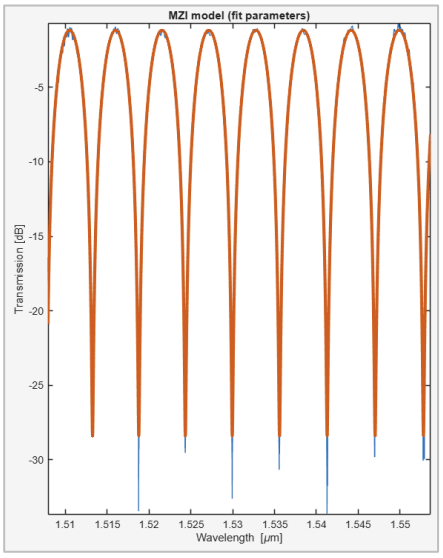

Fig. 14. Final fit. The fit parameters obtained here can be used to calculate all the required parameters.

As a final step we will plot the group index vs wavelength based on the fit parameters. This is shown in figure 15.

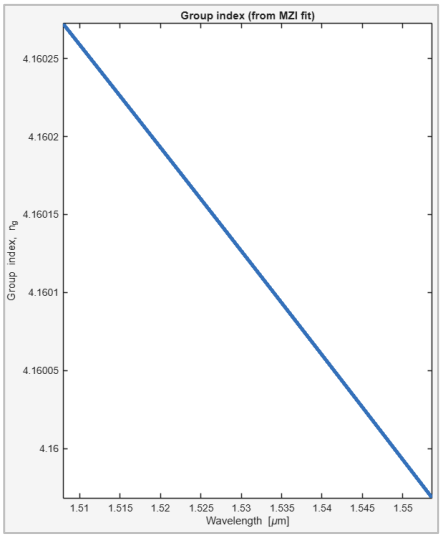

Fig. 14. Group index vs wavelength obtained via the fit parameters.

The FSR and group index extracted from this process are 5.64 nm and 4.16. We can compare this to the theoretical FSR reported in table III which is 5.72 nm for the 100 um delay circuit and see that it is a very good match.

The extracted values for FSR and group index for each of the measured circuits are shown in table IV all of which closely match the theoretical values calculated.

TABLE IV
MEASURED/EXTRACTED CIRCUIT PARAMETERS

CIRCUIT NAME	GROUP INDEX	FSR (NM)
FARHADM_MZI251	1.045	22.44
FARHADM_MZI252	1.047	22.36
FARHADM_MZI253	1.040	22.43
FARHADM_MZI501	2.093	10.99
FARHADM_MZI502	2.091	10.97
FARHADM_MZI503	2.085	11.27
FARHADM_MZI1001	4.184	5.61
FARHADM_MZI1002	4.160	5.64

REFERENCES AND FOOTNOTES

[1] Edmund Optics, “Building a Mach-Zehnder Interferometer,” Knowledge Center, 2016. [Online]. Available: https://www.edmundoptics.com/knowledge-center/application-notes/optomechanics/building-a-mach-zehnder-interferometer/

[2] edX, “PHOT1x: Introduction to Photonics,” course lecture slides, 2025.

[3] R. J. Bojko, J. Li, L. He, T. Baehr-Jones, M. Hochberg, and Y. Aida, "Electron beam lithography writing strategies for low loss, high confinement silicon optical waveguides," J. Vacuum Sci. Technol. B 29, 06F309 (2011)

[4] Lukas Chrostowski, Michael Hochberg, chapter 12 in "Silicon Photonics Design: From Devices to Systems", Cambridge University Press, 2015

[5] http://siepic.ubc.ca/probestation, using Python code developed by Michael Caverley.

[4] Yun Wang, Xu Wang, Jonas Flueckiger, Han Yun, Wei Shi, Richard Bojko, Nicolas A. F. Jaeger, Lukas Chrostowski, "Focusing sub-wavelength grating couplers with low back reflections for rapid prototyping of silicon photonic circuits", Optics Express Vol. 22, Issue 17, pp. 20652-20662 (2014) doi: 10.1364/OE.22.020652

[6] www.plcconnections.com, PLC Connections, Columbus OH, USA.

[7] http://mapleleafphotonics.com, Maple Leaf Photonics, Seattle WA, USA.

ACKNOWLEDGMENT

We acknowledge the edX UBCx Phot1x Silicon Photonics Design, Fabrication and Data Analysis course, which is supported by the Natural Sciences and Engineering Research Council of Canada (NSERC) Silicon Electronic-Photonic Integrated Circuits (SiEPIC) Program. The devices were fabricated by Richard Bojko at the University of Washington Washington Nanofabrication Facility, part of the National Science Foundation’s National Nanotechnology Infrastructure Network (NNIN), and Cameron Horvath at Applied Nanotools, Inc. Omid Esmaeeli performed the measurements at The University of British Columbia. We acknowledge Lumerical Solutions, Inc., Mathworks, Mentor Graphics, Python, and KLayout for the design software.